

REPORT No. 430

MEASUREMENTS OF FLOW IN THE BOUNDARY LAYER OF A 1/40-SCALE MODEL OF THE U. S. AIRSHIP "AKRON"

BY HUGH B. FREEMAN

SUMMARY

This report presents the results of measurements of flow in the boundary layer of a 1/40-scale model of the U. S. airship "Akron" ("ZRS-4") made with the object of determining the boundary-layer thickness, the point of transition from laminar to turbulent flow, and the velocity distribution in the boundary layer.

The boundary-layer thickness was found to vary along the 19.62-foot hull from 0.08 inch at the most forward station, about 15 inches from the nose, to approximately 10 inches at the tail. A marked increase in the rate of thickening of the boundary layer was found at the transition from laminar to turbulent flow which occurred at

a Reynolds Number $\left(\frac{Va}{\nu}\right)$ of about 814,000, where (a) is the axial distance from the nose. The velocity distribution over the greater part of the turbulent portion of the boundary layer was found to be fairly well approximated by the seventh-power law. The frictional drag, computed from the loss of momentum in the boundary layer and also from Clark Millikan's equations, was in good agreement with the measured drag.

INTRODUCTION

Measurements in the boundary layers of streamline bodies have shown that the flow, similar to that over flat plates placed edgewise to the air stream, is laminar for a certain distance from the nose, then becomes turbulent, and that the velocity distribution in the laminar and turbulent portions is similar to that deduced by Blasius and Von Karman, respectively. (References 1 and 2.)

The point of transition from laminar to turbulent flow is of great interest in the study of the drag of streamline bodies since its variation with Reynolds Number and with the initial degree of turbulence in the air stream approaching the body has been shown by Jones (reference 3) and by Dryden and Kuethe (reference 4) to be largely responsible for the wide difference found in measurements of the drag of different airship models and of the same model in different wind tunnels. The velocity distribution and

the extent of the boundary layer are of interest in verifying equations, such as those of Clark Millikan (reference 5), derived to account for the skin friction of streamline bodies in axial flow.

The subject tests, which were undertaken in conjunction with the measurements of (1) the forces and moments on the hull, (2) the elevator forces and hinge moments, and (3) the pressure distribution over the hull and fins of a 1/40-scale model of the *Akron* (reference 6), were made with the object of determining the velocity distribution in the boundary layer, the extent of the boundary layer, and the point of transition from laminar to turbulent flow. The frictional drag, as computed from considerations of the changes of momentum in the boundary layer and from Millikan's equations, is also presented and compared to the measured drag.

Two advantages are offered by the large size of the model and by the N. A. C. A. 20-foot propeller-research tunnel in which the tests were conducted. The first is that the boundary-layer test apparatus may be rigidly attached to the interior of the model, allowing greater accuracy in the measurement of distances than is possible by the method of mounting the apparatus separately and approaching the model through the wind stream from the outside. The second is that the tests may be made at a Reynolds Number considerably higher than any previously obtained in tests of a similar nature.

APPARATUS AND TESTS

The airship model, shown in Figure 1 mounted in the propeller-research wind tunnel, is of hollow wooden construction having 36 sides over the forepart of the hull that faired into 24 sides near the stern. The surface was given a fine sand finish, then varnished, painted, and finally finished with fine sandpaper, giving a surface which was probably as smooth as that of a well-doped fabric surface. The length of the model is 19.62 feet, the maximum diameter 3.32 feet, and the fineness ratio 5.9.

The tube and accessory apparatus used in measuring the total head in the boundary layer are shown in

Figure 2. The apparatus was bolted to the interior structure of the hull in a manner such that the total-head tube shaft, which passed through a small opening in the hull of the model, was normal to the surface. A motor-driven screw thread governed the distance of the total-head tube from the hull and operated, by means of an eccentric and contactor, an electric counter which gave this distance directly in thousandths of an inch. The end of the total-head tube, fashioned from a copper tube whose outside diameter was approxi-

the surface of the hull at each station at which the measurements were made.

A small hole, drilled into the brass plate, adjacent to the total-head tube, served as an orifice at which the static pressure was measured. Both the total-head tube and the static-pressure orifice were connected to micromanometers in the test chamber below.

Measurements of the total head and of the static pressure were made at 10 stations along the hull spaced approximately 2 feet apart. The location of the

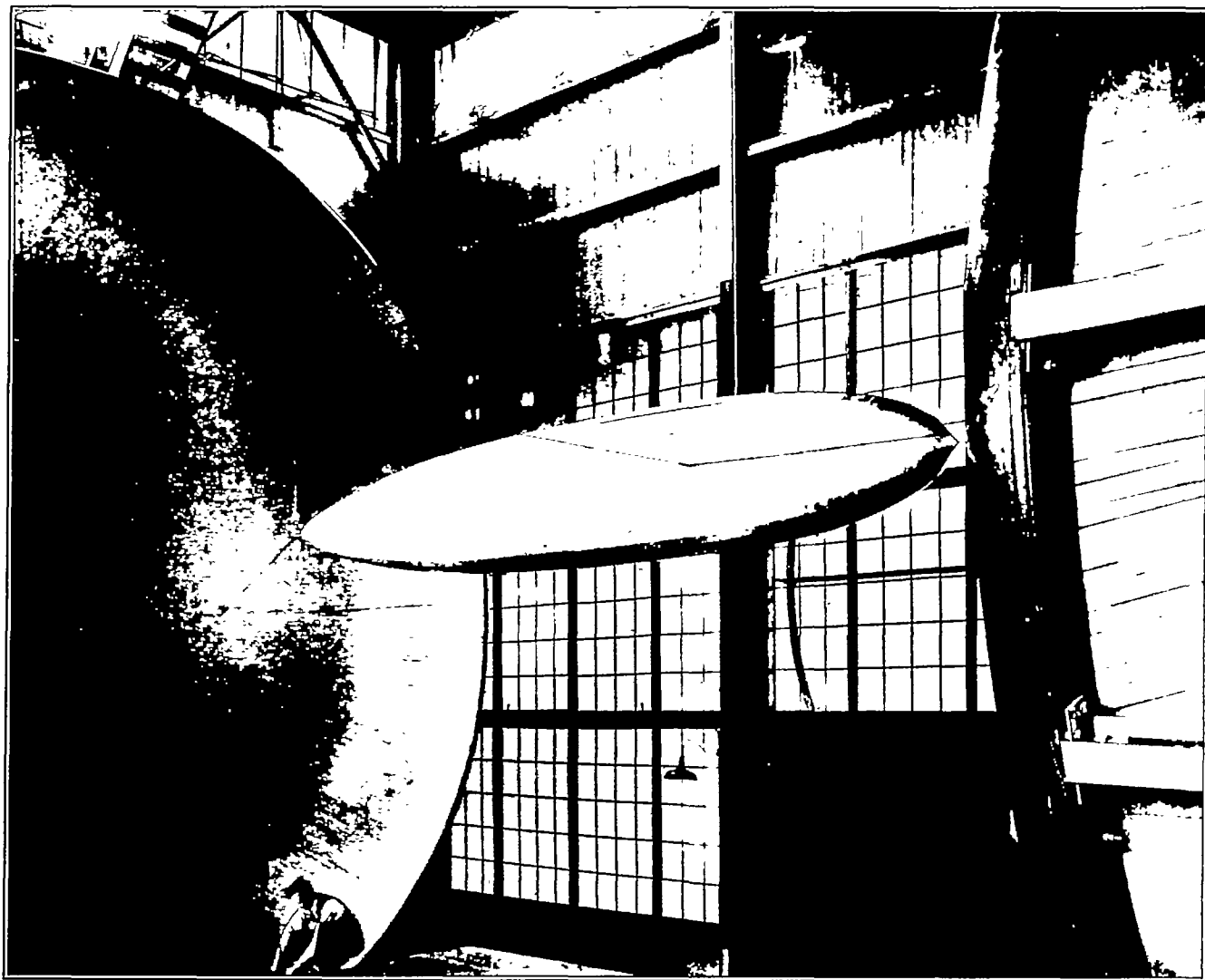


FIGURE 1.—Airship model *Akron* mounted in wind tunnel

mately 0.02 inch, was pressed into a rectangular shape with a depth of opening of 0.0034 inch. The wall thickness was ground down to 0.0032 inch so that when the tube was in contact with the surface of the hull the distance from the center of the opening to the hull was 0.0049 inch.

Contact between the total-head tube and the surface of the hull was indicated by the lighting of a neon bulb which was connected in series with the total-head tube and a brass plate set into, and flush with,

stations is shown in Figure 3. A total-head survey, to determine the depth of the boundary layer only, was also made at an additional station near the tail of the model with a $\frac{1}{8}$ -inch copper tube supported from outside the wind stream.

The test procedure was to take the first reading with the tube touching the hull and then to move away from the hull in 0.001-inch steps, taking readings each time out to 0.015 inch from the hull. The length of the steps was then increased gradually until the tube

approached the limit of the boundary layer, where the distance between observation points was decreased again. Tests were made at three values of the dynamic pressure ($q = 12.5, 19, \text{ and } 25.6$ pounds per square foot)

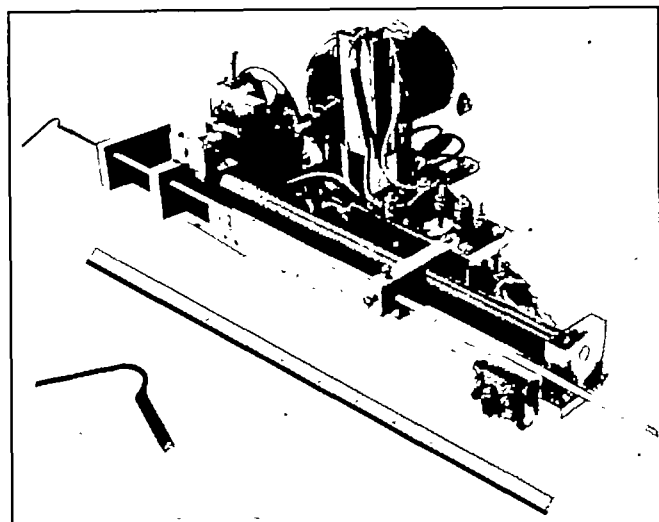


FIGURE 2.—Apparatus used for measuring total head in the boundary layer—airship model Akron

corresponding to velocities of approximately 70, 86, and 100 miles per hour, respectively.

PRECISION

The maximum departure of the observed wind-tunnel velocity from a mean value was about ± 0.6 per cent. The accuracy in the outer portion of the boundary layer was about ± 1 per cent but decreased rapidly for values in the inner portion.

A calibration of the total-head tube against a standard Prandtl-type tube showed that its readings were about 2 per cent low over the range of speeds of these tests. The calibration, made with increasing speeds and again with decreasing speeds, showed no appreciable time lag.

with the hull. A second error of ± 0.002 inch is possible because the brass plates set into the hull at each station may not have been exactly flush with the surface. A third small error is possible owing to the fact that the velocity computed from the pressure at the mouth of even a very small tube, placed in a velocity gradient, is not necessarily the same as that at the geometrical center of the tube. (Reference 7.)

Although these inaccuracies eliminate the possibility of determining the intensity of friction from the slope of the velocity curve at the surface of the hull, they are negligible in the determination of this quantity from the changes of momentum in the boundary layer and in the determination of the boundary-layer thickness except at the most forward position, where the layer is very thin.

RESULTS AND DISCUSSION

The observed results of the measurements of the total head, the dynamic head, and the velocity in the boundary layer are presented in Table I. The total head and the dynamic pressure are given in terms of the dynamic pressure in the free air stream, the velocity as a fraction of the velocity just outside the boundary layer at the particular station in question. The values for the ratio of the velocity in the boundary layer to that just outside the boundary layer are plotted for all of the stations in Figure 4.

The total head in the boundary layer increases with the distance from the surface until it eventually approaches a constant value. The distance from the hull (y) at which this occurred has been designated as the boundary-layer thickness δ . An estimate of this value was made by fairing the results. The total-head values were first plotted against the distance from the hull and the limiting value to which the curve tended was determined. The value of y at which the total head became equal to this limiting value was then determined for each station and plotted against the

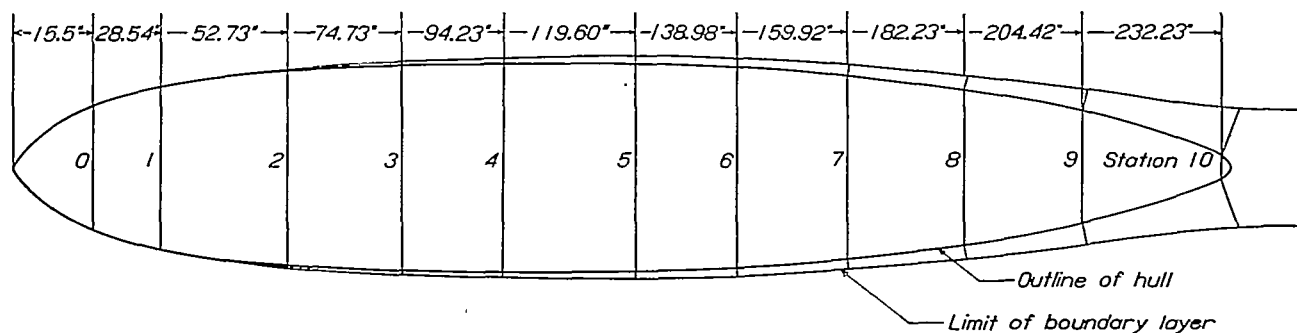


FIGURE 3.—Location of stations at which boundary-layer measurements were made—airship model Akron

The relative distances y of the total-head tube from the hull are considered in general as accurate as the screw which governed this distance. The absolute distance, however, may be in error as much as ± 0.001 inch because the electrical system was not sensitive enough to indicate exactly when the tube made contact

distance along the axis. Since there appeared to be no consistent difference in the thickness for the three speeds a mean value was determined for each station. These values are plotted in Figure 4. The boundary-layer thickness varies along the 19.62-foot hull from 0.08 inch at the most forward station to approximately

10 inches at the extreme tail. The variation is approximately linear over about 60 per cent of the length, but increases very rapidly over the after portion of the hull as the cross section of the hull decreases.

A sudden increase in the boundary-layer thickness was found to occur between stations 0 and 1. In experiments on flat plates such an increase in thickness was found to occur in the region of transition from laminar to turbulent flow. (References 8 and 9.) Previous experiments on airship forms, however, have not shown this phenomenon. (References 1 and 2.) Further evidence of a transition is shown by the plot of the curves of velocity distribution in Figure 5.

The curve for the low speed falls closer to the laminar curve than the one for the high speed. The Reynolds Number ($\frac{Va}{\nu} = 814,000$, where V is the free-stream velocity and a is the axial distance from the nose) for this position at the low speed is in agreement with the results of Ower and Hutton who found a transition to occur between values of 570,000 and 940,000. (Reference 2.)

The values of u/u_s are shown in Figure 6 plotted on logarithmic paper against values of y/δ for 5 stations. The points fall on a slightly sinuous curve which may be fairly well approximated by a straight line, that is,

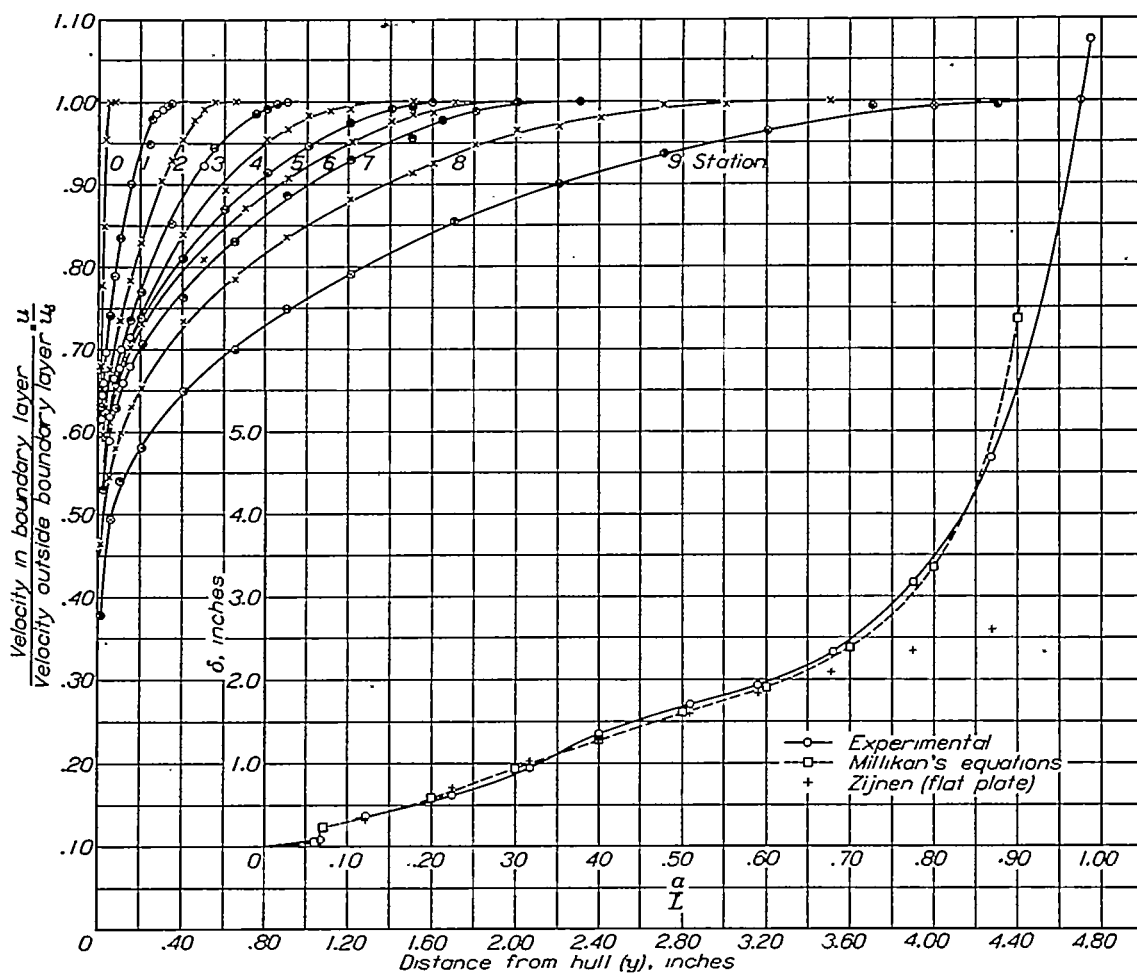


FIGURE 4.—Velocity distribution in the boundary layer and boundary-layer thickness along the hull—airship model Akron

The curves for all of the stations, with the exception of the most forward position (station 0) approximate the form which is characteristic of turbulent flow. Curves for both the high and low speeds have been plotted for position 0. The results for the intermediate speed which are practically the same as those for the high speed are not shown. These curves resemble more closely that typical of laminar flow, the approximate form of which is also shown. The form of these curves and the fact that the curves for the two speeds do not agree indicates that the flow at this position is not strictly laminar but has already started to change.

by an equation of the form $u/u_s = (y/\delta)^{1/n}$, except for that portion of the curve for which the tube was very close to the hull. The values of n vary from 6.4 at station 1 to 7.2 at station 5 and decrease again to 6.2 at station 9. For the stations 4 to 8, inclusive, the value of n is approximately 7. This region corresponds to that of low curvature of the hull and of low static-pressure gradient in the tunnel. A small increase in the value of n was observed with an increase in velocity.

The average values of the static pressure measured at the various stations are plotted in Figure 7 and

compared to the average pressures about the hull determined by pressure-distribution tests (results not yet published). The two sets of values are in good agreement except in the critical region at station

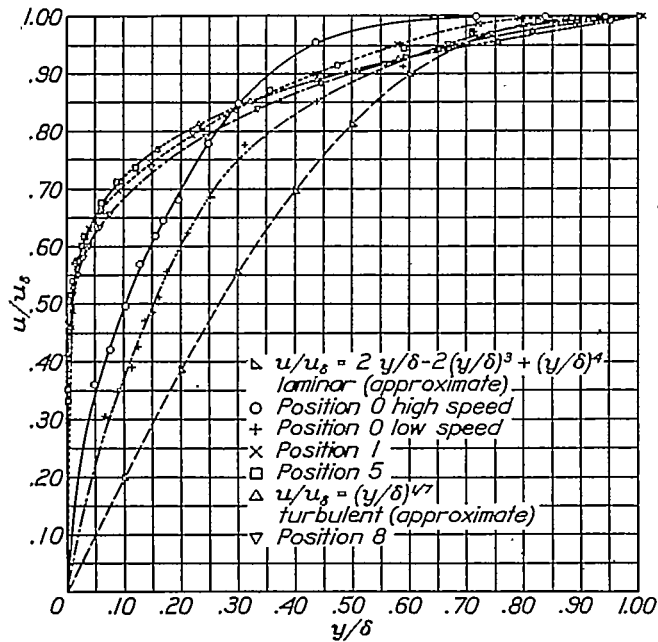


FIGURE 5.—Velocity distribution for laminar and turbulent portions of boundary layer—airship model Akron

0. The values plotted are the pressures measured with reference to the static pressure in the test chamber and have not been corrected for the tunnel walls or

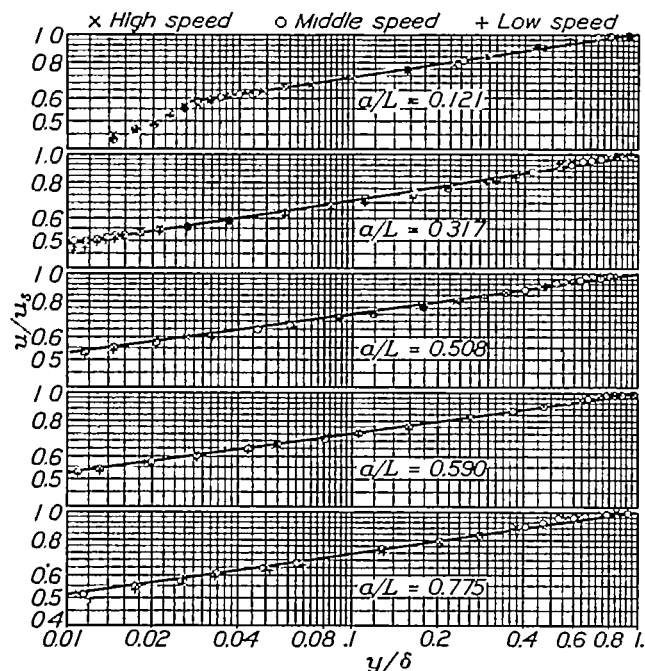


FIGURE 6.—Logarithmic plot of velocity distribution—airship model Akron

the variation of the static pressure along the axis of the air stream. This variation is given in the following table.

a/L	0	0.1	0.2	0.3	0.4	0.5	0.6	0.7	0.8	0.9	1.0
P/q_s	.032	.025	.020	.017	.015	.013	.011	.010	.010	.011	.013

ESTIMATION OF SURFACE FRICTION FROM MOMENTUM IN THE BOUNDARY LAYER

A consideration of the changes in momentum of the air in the boundary layer as it flows around the airship hull allows the surface friction to be evaluated. The equation for the frictional intensity is

$$\frac{r_o f}{2} = \frac{d}{dx} \int_0^s (H_s - H) r dy - \sqrt{q_s} \frac{d}{dx} \int_0^s (\sqrt{q_s} - \sqrt{q}) r dy$$

where f —frictional intensity.

H —total head in the boundary layer.

H_s —total head just outside boundary layer.

q_s —dynamic pressure outside boundary layer.

q —dynamic pressure inside boundary layer.

r_o —radius of hull.

$r = r_o + y \cos \alpha$.

α —inclination of hull to the axis.

y —distance normal to hull.

x —distance along surface measured from nose.

The method of derivation of this equation is similar to that used by Von Karman (reference 10, see also refer-

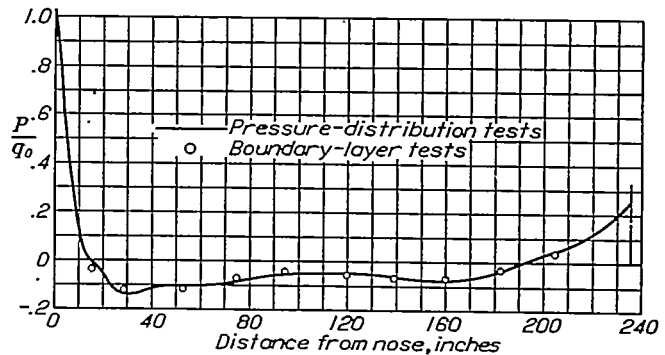


FIGURE 7.—Average pressures about hull from pressure distribution tests compared to static pressure measured along one longitudinal in boundary-layer tests—airship model Akron

ence 4) for the 2-dimensional case and has therefore been omitted. The form of the equation given above (suggested by Ira H. Abbott of this laboratory) is more convenient for the numerical computations than the alternate form for this equation derived by Clark Millikan (reference 5) in a different manner. It should be noted that, in the derivation of the equation given above, the assumption has been made that the pressure at any point in the boundary layer, for any given section, is the same as the pressure measured at the surface of the hull at that section.

The results of the two integrations, determined graphically for each station, are plotted in Figure 8 against the distance x and the resulting curves are designated A and B. These curves are differentiated graphically and the equation solved for the frictional intensity (f/q_o) and for the frictional drag per foot run of surface ($\frac{2\pi r_o f}{q_o} \cos \alpha$). These values and the

velocity coefficients (u_s/V) for the different stations are also shown in Figure 8. The frictional intensity is a maximum at about 2 feet from the nose of the hull. A second smaller maximum occurs on the after portion of the hull about 14 feet from the nose. Because of the scattering of the test points on the after portion of the hull, however, the shape of the curve in this region is not at all certain.

taneously. This is the reason for the discontinuity in curve D near the nose of the model.

The frictional force on any small element of surface area may be divided into two components normal and parallel, respectively, to the hull axis. The integrated components parallel to the axis constitute the frictional drag and enter directly into the forces measured on the wind-tunnel balances. The components of

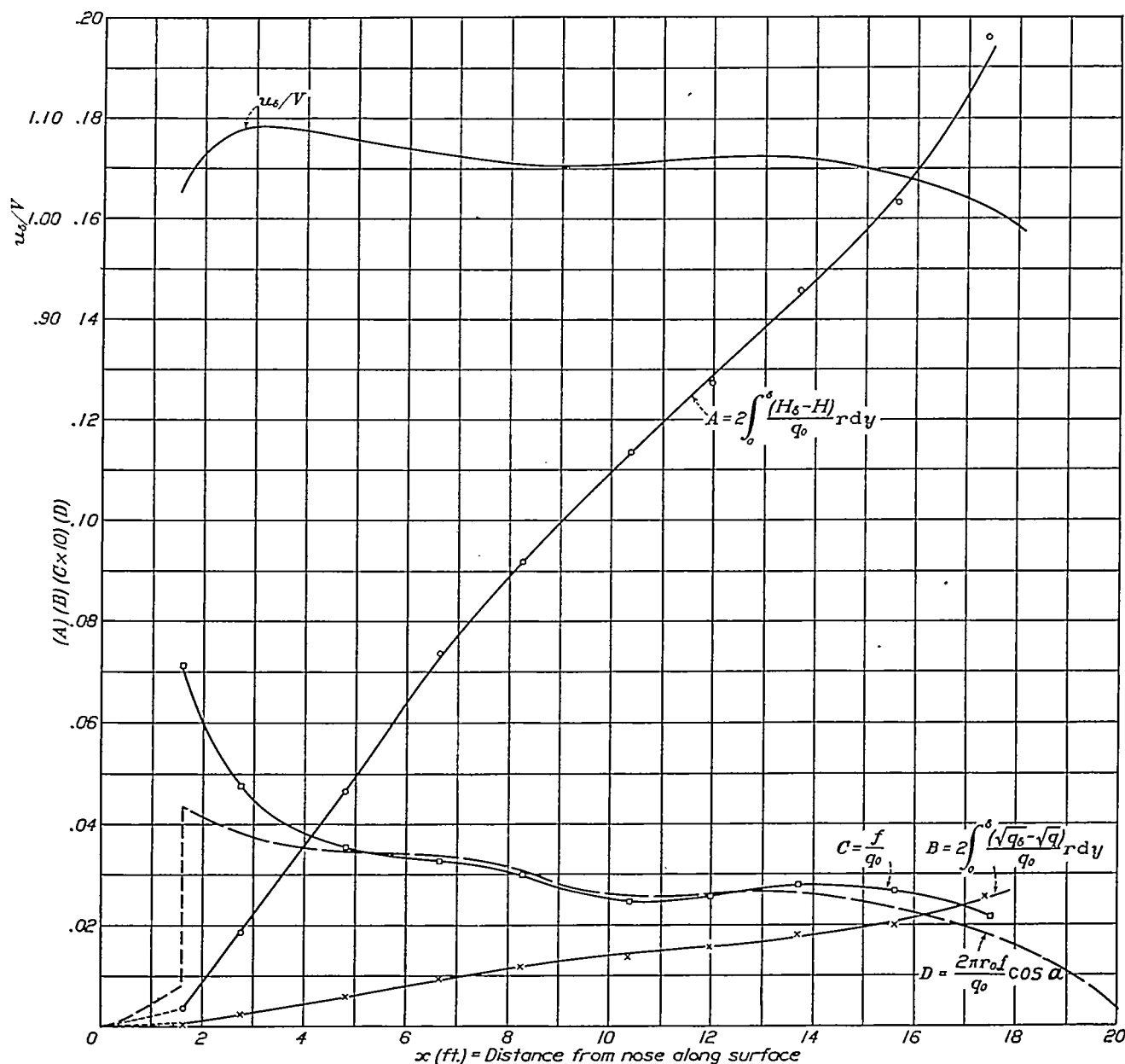


FIGURE 8.—Frictional drag determined from loss of momentum in the boundary layer—airship model Akron

Because of the lack of experimental data over the nose of the hull, the portion of curve D corresponding to the laminar flow over the nose was computed from Clark Millikan's equations which are discussed later in this report and, as it is not known how the transition actually takes place, it was assumed to occur instan-

the forces normal to the axis have equal and opposite components on the opposite sides of the hull, at the same section, and consequently the integrated resultant of these forces is zero. However, since these frictional forces represent a loss of energy in the air stream, they must give rise to a pressure drag. Pressure-distribu-

tion tests have shown that the measured drag on the present model is so small as to be negligible.

The following table gives a comparison of the integrated frictional drag and the measured drag for the three speeds tested. The values listed are the usual coefficients based on the volume to the two-thirds power.

Dynamic pressure of free stream, q_∞ -----	12.5	19.0	25.6
Integrated frictional drag, C_f -----	.0219	.0214	.0207
Measured drag (from force tests), C_d -----	.0198	.0193	.0190

COMPUTATION OF FRICTIONAL DRAG BY MILLIKAN'S EQUATIONS

For the derivation and discussion of the equations used in the following computations the reader is referred to reference 5. In these equations for the boundary-layer thickness and the frictional drag of laminar and turbulent portions of the boundary layer the velocity distribution was assumed to be of the form

$$u/u_\delta = a + b\left(\frac{y}{\delta}\right) + c\left(\frac{y}{\delta}\right)^2$$

for the laminar flow, where a , b , and c were constants determined by the conditions at the boundaries, and the equation

$$u/u_\delta = \left(\frac{y}{\delta}\right)^{1/7}$$

was assumed to hold for the turbulent portion. The first assumption, about which the data of the subject tests do not give any definite information, is of secondary interest for Reynolds Numbers equal to or greater than those of the present tests because of the fact that only a small portion of the boundary layer is laminar. The second assumption, as far as the present tests are concerned, has been shown to be in fair agreement with the experimental results.

The equations for the laminar flow are:

$$\left. \begin{aligned} \text{boundary-layer thickness} &= \frac{\delta_l}{L} = \frac{\sqrt{30}}{R^{1/2}} M\left(\frac{a}{L}\right) \\ \text{boundary-layer Reynolds Number } R_{\delta_l} &= \frac{u_\delta \delta_l}{\nu} = \sqrt{30} R^{1/2} \left(\frac{u_\delta}{V}\right) M\left(\frac{a}{L}\right) \\ \text{where } M\left(\frac{a}{L}\right) &= \frac{1}{\left(\frac{u_\delta}{V}\right)^{9/2} r_o} \left[\int_0^{a/L} \frac{\left(\frac{u_\delta}{V}\right)^8 \left(\frac{r_o}{L}\right)^2}{\beta} d\left(\frac{a}{L}\right) \right]^{1/4} \end{aligned} \right\} (1)$$

The frictional-drag coefficient for laminar flow is—

$$C_{f,l} = \frac{4.59}{R^{1/2}} \frac{L^2}{(Vol)^{2/3}} \int_0^{a/L} \frac{\frac{u_\delta}{V} \cdot \frac{r_o}{L}}{M\left(\frac{a}{L}\right)} d\left(\frac{a}{L}\right) \quad (2)$$

where a —distance from nose measured along the axis.
 L —length of model.

R —Reynolds Number $\frac{VL}{\nu}$.

δ_l —thickness of laminar boundary layer.

V —velocity of free air stream.

a_c —critical value of a at the transition point.

Vol—volume of airship hull.

$\beta = \cos \alpha$.

α —inclination of hull to axis.

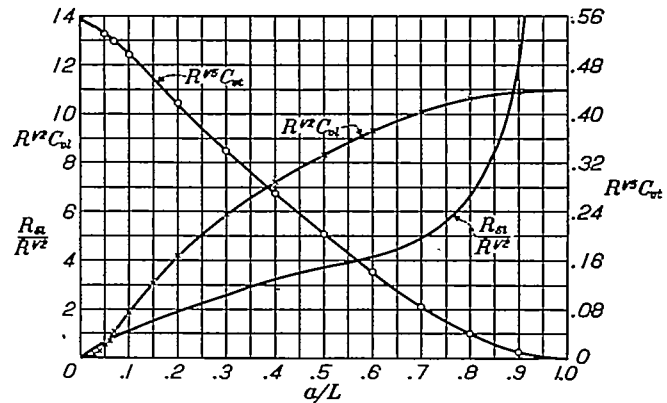


FIGURE 9.—Contribution of laminar and turbulent portions of boundary layer to frictional drag (Millikan's equations)—airship model Akron

For turbulent flow: The boundary-layer thickness is—

$$\frac{\delta_t}{L} = \frac{0.370}{R^{1/5}} N\left(\frac{a}{L}, \frac{a_c}{L}\right)$$

and boundary-layer Reynolds Number $R_{\delta_t} = \frac{u_\delta \delta_t}{\nu}$ (3)

$$= 0.370 R^{1/5} \left(\frac{u_\delta}{V}\right) \cdot N\left(\frac{a}{L}, \frac{a_c}{L}\right)$$

where

$$N\left(\frac{a}{L}, \frac{a_c}{L}\right) = \frac{1}{\left(\frac{u_\delta}{V}\right)^{23/7} r_o} \left[\int_{a_c/L}^{a/L} \frac{\left(\frac{u_\delta}{V}\right)^{27/7} \left(\frac{r_o}{L}\right)^{5/4}}{\beta} d\left(\frac{a}{L}\right) + 3.46 R^{1/4} \left(\frac{\delta_{ct}}{L}\right)^{5/4} \left(\frac{u_\delta}{V}\right)^{115/28} \left(\frac{r_{oc}}{L}\right)^{5/4} \right]^{1/5} \quad (4)$$

The frictional-drag coefficient for turbulent flow is—

$$C_{f,t} = \frac{0.3625}{R^{1/5}} \frac{L^2}{(Vol)^{2/3}} \int_{a_c/L}^{a/L} \frac{\left(\frac{u_\delta}{V}\right)^{7/4} \frac{r_o}{L}}{N^{1/4}} d\left(\frac{a}{L}\right) \quad (5)$$

where δ_t —turbulent boundary-layer thickness and subscript c indicates critical value at transition point.

The total frictional-drag coefficient then equals—

$$C_f = C_{f,l} + C_{f,t}$$

In order to simplify the computations it has been assumed that the transition was instantaneous and that the flow behind the transition acted just as though the entire boundary had been turbulent from the nose

of the hull. The result of this assumption is that the second term in equation (4) disappears, leaving N as a function of one variable $\left(\frac{a}{L}\right)$ instead of two. The data used in these computations are given in the following table.

a/L	r_a/L	β	u_0/V
0	0	0.655	0
0.01	0.0090	.655	0.480
.02	.0210	.639	.710
.03	.0297	.759	.855
.04	.0387	.850	.947
.05	.0423	.900	.995
.06	.0470	.921	1.024
.07	.0503	.935	1.042
.10	.0603	.965	1.076
.15	.0707	.987	1.093
.20	.0781	.995	1.098
.25	.0812	.998	1.075
.30	.0823	1.000	1.066
.35	.0843	1.000	1.053
.40	.0845	1.000	1.053
.45	.0845	1.000	1.053
.50	.0841	1.000	1.054
.55	.0832	1.000	1.057
.60	.0812	.999	1.060
.65	.0784	.998	1.061
.70	.0743	.995	1.060
.75	.0686	.992	1.053
.80	.0613	.988	1.041
.85	.0523	.979	1.021
.90	.0403	.970	.986
.95	.0377	.953	.931
1.00	0	0	0

$L=19.62$ feet.
(Vol)^{1/3}=23.65 sq. ft.

The values of boundary-layer thickness computed from equations (1) and (3) are compared to the experimental values in Figure 4. The computed value for position 0 is seen to be lower than the experimental value. This difference may, possibly, be accounted for by the fact, previously mentioned, that the flow at this position was not entirely laminar and the boundary had already begun to thicken. If the thickness is computed using the equation—

$$\delta = 5.5 \sqrt{\frac{\nu x}{u_s}}$$

which is used to define the boundary for 2-dimensional laminar flow, a value is obtained ($\delta=0.083$ inch) which is in very good agreement with the experimental value. The values for the turbulent flow are in good agreement over the hull except near the tail where both the theoretical and the experimental results are less accurate. The boundary was also computed for the turbulent flow by use of the equation—

$$\delta = 0.37(x - x_0)^{4/5} \left(\frac{\nu}{u_s}\right)^{1/5}$$

where x_0 distance, along the surface, from the nose to the point of transition. This is an extension (Zijnen, reference 8) of Prandtl's equation for flat plates. These values (fig. 4) are in close agreement with the experimental values up to 60 per cent of the length of the hull. Over the after portion of the hull, however, the computed values are much too low.

The contributions of the laminar and turbulent flow to the frictional drag $R^{1/2}C_{f,i}$ and $R^{1/2}C_{f,t}$ were computed from equations (2) and (5), respectively, and are shown in Figure 9 plotted against the ratio a/L .

By assuming a value of $R_{\delta,i}$ at which the transition takes place, values of a/L , $R^{1/2}C_{f,i}$, and $R^{1/2}C_{f,t}$ may be taken from the curves and the frictional drag of the model computed for any range of the Reynolds Number, R . The transition curve for the Akron model was computed in this way, assuming a value of $R_{\delta,i}=3,620$ corresponding to the experimentally determined value of $a/L=0.07$ for the critical point at which the laminar flow breaks down. This curve and the curves for the limiting cases where the flow is entirely laminar and entirely turbulent are shown in Figure 10 compared to the measured drag of the model. For the limiting cases the equations $C_{f,i}=10.95R^{-1/2}$ and $C_{f,t}=0.554R^{-1/2}$, obtained by assuming critical values of $\frac{a_c}{L}=1$ and $\frac{a_c}{L}=0$, respectively, were used. The

abscissas here are not $R=\frac{\rho VL}{\mu}$ but $R_s=\frac{\rho V(\text{Vol})^{1/3}}{\mu}$

since most of the experimental results are given in terms of the latter quantity. The computed transition curve is seen to be in very good agreement with the measured results. The fact that they are almost in exact agreement is probably fortuitous.

The results of drag measurements in the variable-density tunnel on two models of the Akron are also shown in Figure 10. The wooden model, 1/200-scale, of polygonal cross section was similar to the model used for the subject tests. (See reference 11.) The second model, for which the results have not yet been published, was of circular cross section, metal, and 1/250-scale.

As previously mentioned in this discussion, the theoretical equations used in the above computations were based on the assumption that the velocity distribution, for the turbulent boundary layer, is approximated by the seventh-power law. Although this has been shown to be true for the present model tests, there are no experimental data available to show that it is true for the Reynolds Number of the full-scale airship. If it could be shown that the velocity distribution in the latter case was approximated by a simple power law, the above theoretical equations, or similar ones, would offer a reliable method of predicting the drag of full-scale airship hulls. It is therefore recommended that this research be extended to include boundary-layer tests, similar in nature to those of the present tests, on the full-scale airship.

CONCLUSIONS

1. The boundary-layer thickness was found to vary along the 19.62-foot hull from 0.08 inch at the most forward station to about 10 inches at the tail.

2. A transition, evidenced by a marked increase in the rate of thickening of the boundary layer and by a change in the character of the velocity distribution was found to occur about 15 inches from the nose of the hull.

3. The velocity distribution was found to be approximated fairly well by an equation of the form $u/u_s = (y/\delta)^{1/n}$ where n is approximately 7 over the central portion of the hull but decreases to 6.4 and 6.2 near the forward and after extremities, respectively.

4. The frictional drag computed from the loss of momentum in the boundary layer and from Clark

3. Jones, B. M.: Skin Friction and the Drag of Streamline Bodies. R. & M. No. 1199, British A. R. C., 1928.
4. Dryden, H. L., and Kuethe, A. M.: Effect of Turbulence in Wind-Tunnel Measurements. T. R. No. 342, N. A. C. A., 1930.
5. Millikan, Clark B.: The Boundary Layer and Skin Friction for a Figure of Revolution. A. S. M. E., Trans. Vol. 54, No. 2, 1932.

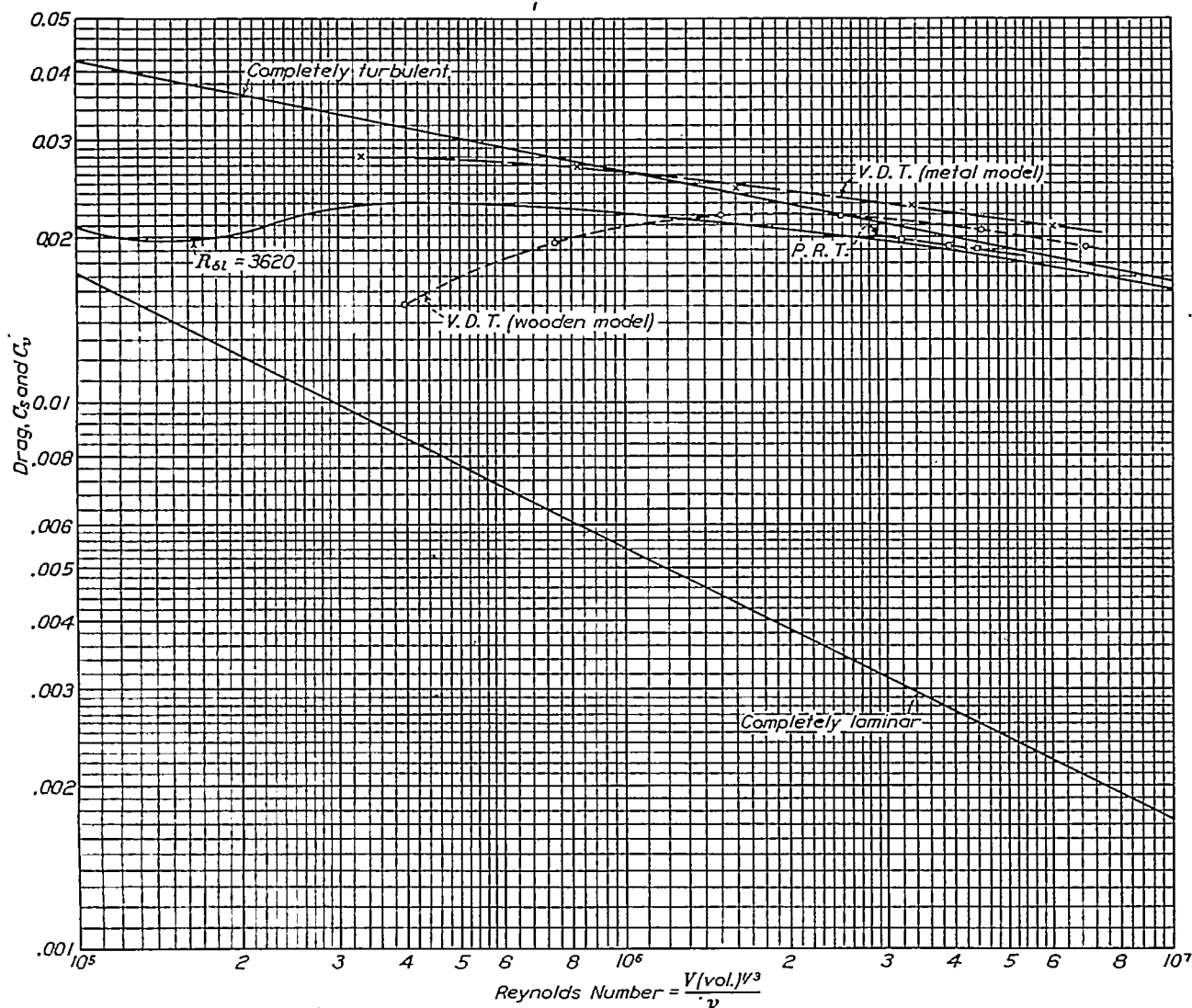


FIGURE 10.—Comparison of computed frictional drag (Millikan's equations) and experimental results—airship model Akron

Millikan's equations was in good agreement with experimental results.

LANGLEY MEMORIAL AERONAUTICAL LABORATORY,
NATIONAL ADVISORY COMMITTEE FOR AERONAUTICS,
LANGLEY FIELD, VA., April 27, 1932.

REFERENCES

1. Simmons, L. F. G.: Experiments Relating to the Flow in the Boundary Layer of an Airship Model. R. & M. No. 1268, British A. R. C., 1929.
2. Ower, E., and Hutton, C. T.: Investigation of the Boundary Layers and the Drags of Two Streamline Bodies. R. & M. No. 1271, British A. R. C., 1929.
3. Freeman, Hugh B.: Force Measurements on a 1/40-Scale Model of the U. S. Airship Akron. T. R. No. 432, N. A. C. A., 1932.
4. Fage, A., and Falkner, V. M.: An Experimental Determination of the Intensity of Friction on the Surface of an Airfoil. R. & M. No. 1315, British A. R. C., 1930.
5. Burgers, J. M., and Zijnen, B. G.: Preliminary Measurements of the Distribution of the Velocity of a Fluid in the Immediate Neighborhood of a Plane, Smooth Surface. Jour. Inst. Aero. Engineers (Great Britain), April, 1927.
6. Hansen, M.: Velocity Distribution in the Boundary Layer of a Submerged Plate. T. M. No. 585, N. A. C. A., 1930.
7. Von Karman, Theodore: Über Laminare und Turbulente Reibung. Zeit. f. Ang. Math. u. Mech. Vol. I, Aug., 1921.
8. Abbott, Ira H.: Airship Model Tests in the Variable Density Wind Tunnel. T. R. No. 394, N. A. C. A., 1931.

TABLE I
BOUNDARY-LAYER DATA FOR MODEL OF U. S. S. "AKRON"

STATION 0

$$a/L=0.066$$

$$\delta=0.080 \text{ inch}$$

Average $q_\infty=25.6 \text{ lb./sq. ft.}$				$q_\infty=19.0 \text{ lb./sq. ft.}$				$q_\infty=12.5 \text{ lb./sq. ft.}$			
y inch	H q_∞	q q_∞	u u_1	y inch	H q_∞	q q_∞	u u_1	y inch	H q_∞	q q_∞	u u_1
0.005	0.082	0.139	0.359	0.005	0.076	0.122	0.335	0.005	0.066	0.113	0.325
.006	.083	.140	.360	.006	.092	.145	.367	.006	.061	.104	.311
.007	.103	.168	.384	.007	.110	.168	.395	.007	.078	.131	.349
.008	.136	.190	.421	.008	.137	.179	.407	.008	.086	.137	.358
.009	.166	.233	.465	.009	.174	.215	.446	.009	.135	.163	.390
.010	.221	.264	.495	.010	.236	.266	.497	.010	.166	.195	.426
.011	.258	.304	.532	.011	.248	.297	.525	.011	.203	.236	.471
.012	.300	.347	.568	.012	.292	.344	.565	.012	.214	.250	.485
.013	.318	.363	.581	.013	.314	.357	.576	.013	.242	.279	.511
.014	.362	.409	.617	.014	.358	.408	.614	.014	.299	.330	.555
.015	.397	.445	.645	.015	.394	.444	.641	.015	.301	.338	.563
.017	.480	.525	.681	.017	.459	.512	.689	.017	.365	.413	.622
.021	.602	.648	.778	.020	.644	.693	.744	.020	.468	.505	.686
.025	.722	.766	.848	.025	.694	.739	.828	.025	.600	.640	.775
.035	.932	.971	.954	.030	.850	.889	.930	.030	.743	.774	.851
.056	1.033	1.064	.999	.035	.921	.958	.944	.035	.859	.888	.911
.081	1.041	1.078	1.000	.060	1.025	1.060	.991	.047	.978	1.003	.970
.105	1.041	1.077	1.000	.080	1.042	1.075	.999	.057	1.030	1.070	.999
.131	1.041	1.077	1.000	.105	1.041	1.075	.999	.067	1.030	1.061	.997
.155	1.041	1.077	1.000	.131	1.040	1.076	.999	.080	1.032	1.057	.995
.183	1.045	1.086	1.003	.155	1.044	1.077	1.002	.105	1.038	1.067	.999
.207	1.041	1.077	1.002	.203	1.036	1.071	.997	.155	1.036	1.068	1.000
				.256	1.040	1.074	1.000	.213	1.036	1.073	1.001
				.305	1.038	1.074	.998				

STATION 1

$$a/L=0.121$$

$$\delta=0.35 \text{ inch}$$

0.005	0.103	0.232	0.442	0.005	0.084	0.217	0.429	0.005	0.072	0.207	0.417
.006	.106	.251	.438	.006	.121	.255	.454	.006	.091	.225	.436
.007	.153	.284	.456	.007	.136	.273	.480	.007	.124	.260	.473
.008	.198	.333	.529	.008	.162	.329	.528	.008	.174	.307	.509
.009	.243	.376	.562	.009	.225	.366	.547	.009	.210	.348	.541
.010	.283	.385	.566	.010	.256	.391	.574	.010	.246	.378	.565
.011	.277	.406	.581	.011	.276	.407	.588	.011	.255	.394	.575
.012	.297	.427	.598	.012	.292	.419	.596	.012	.257	.409	.587
.013	.302	.432	.599	.013	.302	.434	.606	.013	.298	.423	.596
.015	.322	.454	.615	.014	.313	.445	.612	.014	.310	.436	.605
.017	.343	.473	.630	.015	.320	.452	.619	.015	.327	.463	.624
.020	.369	.498	.645	.017	.332	.465	.627	.018	.345	.474	.634
.025	.392	.522	.660	.020	.370	.498	.650	.020	.365	.490	.643
.035	.448	.582	.697	.025	.400	.529	.669	.025	.393	.525	.666
.055	.528	.659	.741	.035	.440	.571	.694	.035	.451	.577	.698
.080	.622	.750	.789	.055	.522	.652	.742	.056	.530	.660	.746
.105	.700	.835	.834	.087	.625	.753	.800	.080	.614	.746	.793
.155	.834	.966	.897	.106	.690	.818	.831	.105	.703	.838	.840
.205	.954	1.085	.943	.130	.766	.895	.869	.130	.761	.891	.865
.255	1.023	1.151	.979	.155	.831	.957	.900	.162	.850	.979	.911
.280	1.040	1.172	.987	.181	.894	1.018	.928	.180	.895	1.022	.929
.305	1.051	1.183	.991	.205	.939	1.069	.952	.205	.951	1.080	.955
.330	1.060	1.192	.996	.231	.987	1.108	.968	.230	.998	1.123	.974
.355	1.062	1.192	.998	.255	1.012	1.140	.983	.255	1.019	1.146	.981
.405	1.062	1.190	.998	.280	1.028	1.160	.989	.280	1.040	1.162	.992
.505	1.060	1.187	.995	.305	1.043	1.172	.998	.305	1.059	1.186	1.000
.755	1.066	1.180	.994	.355	1.056	1.180	1.001	.355	1.060	1.183	1.000
				.406	1.054	1.177	.997	.406	1.064	1.181	1.000
				.505	1.050	1.164	.993	.505	1.054	1.166	.993
				.755	1.051	1.167	.991	.755	1.056	1.161	.990

STATION 2

$$a/L=0.234$$

$$\delta=0.62 \text{ inch}$$

0.005	0.053	0.164	0.375	0.005	0.040	0.153	0.360	0.005	0.029	0.140	0.345
.006	.061	.174	.396	.006	.046	.159	.369	.006	.030	.142	.350
.007	.094	.206	.425	.007	.060	.179	.391	.007	.066	.179	.391
.008	.137	.248	.461	.008	.108	.219	.431	.008	.105	.215	.423
.009	.172	.284	.494	.009	.149	.261	.470	.009	.140	.252	.464
.010	.207	.317	.523	.010	.171	.283	.491	.010	.175	.287	.496
.011	.207	.318	.524	.011	.210	.328	.528	.012	.196	.308	.513
.012	.230	.340	.541	.012	.229	.347	.544	.013	.212	.324	.527
.013	.244	.356	.554	.013	.227	.339	.537	.014	.220	.331	.533
.014	.246	.358	.556	.014	.240	.352	.546	.015	.230	.341	.540
.015	.258	.370	.564	.015	.251	.362	.555	.017	.251	.362	.557
.017	.272	.383	.575	.017	.262	.374	.564	.020	.271	.384	.576
.020	.284	.395	.583	.020	.281	.394	.578	.025	.301	.415	.596
.025	.304	.417	.597	.025	.305	.414	.593	.035	.329	.442	.616
.035	.346	.461	.625	.035	.349	.459	.624	.055	.396	.510	.661
.055	.415	.530	.675	.055	.399	.512	.659	.081	.465	.589	.688
.080	.463	.581	.708	.080	.462	.575	.698	.109	.510	.624	.731
.105	.517	.635	.736	.105	.509	.625	.730	.131	.549	.664	.755
.155	.598	.716	.784	.130	.544	.663	.749	.155	.581	.698	.775

TABLE I—Continued
STATION 2—Continued

Average $q_o=25.6$ lb./sq. ft.				$q_o=19.0$ lb./sq. ft.				$q_o=12.5$ lb./sq. ft.			
y inch	$\frac{H}{q_o}$	$\frac{q}{q_o}$	$\frac{u}{u_s}$	y inch	$\frac{H}{q_o}$	$\frac{q}{q_o}$	$\frac{u}{u_s}$	y inch	$\frac{H}{q_o}$	$\frac{q}{q_o}$	$\frac{u}{u_s}$
0.205	0.680	0.800	0.839	0.155	0.582	0.700	0.771	0.205	0.660	0.777	0.817
.305	.826	.947	.904	.205	.677	.799	.824	.255	.739	.857	.856
.355	.885	1.005	.928	.255	.756	.877	.864	.305	.809	.928	.891
.405	.943	1.061	.954	.305	.818	.939	.893	.355	.864	.981	.916
.455	.992	1.112	.977	.355	.854	.982	.915	.405	.938	1.053	.950
.505	1.023	1.143	.990	.405	.844	1.060	.950	.455	.981	1.097	.978
.555	1.048	1.160	.999	.455	.893	1.111	.973	.505	1.017	1.133	.986
.655	1.061	1.169	1.001	.505	1.031	1.136	.982	.555	1.044	1.159	.998
.805	1.061	1.167	1.001	.555	1.046	1.161	.998	.605	1.046	1.159	.998
1.005	1.061	1.162	.999	.617	1.059	1.173	.999	.681	1.053	1.163	.999
				.705	1.064	1.173	1.000	.706	1.057	1.166	1.001
				.805	1.060	1.167	.996	.805	1.058	1.167	1.000
				1.005	1.059	1.163	.996	1.005	1.057	1.162	.998

STATION 3

$$a/L=0.317$$

$$\delta=0.95 \text{ inch}$$

0.005	0.095	0.163	0.379	0.005	0.093	0.160	0.375	0.005	0.065	0.136	0.346
.006	.101	.169	.386	.006	.094	.162	.378	.006	.074	.144	.349
.007	.134	.202	.422	.007	.120	.188	.405	.007	.102	.172	.389
.008	.162	.228	.449	.008	.146	.214	.432	.008	.141	.209	.430
.009	.184	.248	.469	.009	.183	.248	.466	.009	.149	.217	.439
.010	.195	.262	.481	.010	.215	.281	.488	.010	.174	.239	.460
.011	.212	.279	.498	.011	.213	.276	.497	.011	.188	.254	.472
.012	.223	.287	.505	.012	.221	.286	.503	.012	.203	.269	.483
.013	.234	.300	.515	.013	.233	.298	.512	.013	.212	.281	.497
.014	.235	.301	.516	.014	.240	.304	.520	.014	.214	.282	.501
.015	.244	.311	.525	.015	.244	.309	.522	.015	.219	.289	.506
.017	.261	.328	.539	.017	.257	.321	.534	.017	.242	.310	.523
.020	.274	.341	.550	.020	.271	.335	.544	.020	.257	.325	.537
.025	.290	.353	.561	.025	.285	.351	.556	.025	.278	.345	.552
.035	.318	.386	.583	.036	.320	.389	.586	.036	.310	.380	.580
.055	.367	.440	.624	.055	.367	.440	.624	.055	.357	.483	.616
.080	.426	.500	.663	.080	.422	.498	.660	.080	.397	.471	.647
.105	.479	.555	.700	.105	.453	.529	.680	.105	.437	.515	.675
.155	.531	.612	.735	.155	.525	.605	.726	.155	.505	.583	.705
.205	.592	.672	.770	.205	.580	.661	.761	.205	.578	.655	.762
.255	.743	.823	.852	.255	.674	.752	.815	.280	.650	.729	.803
.305	.832	.960	.922	.305	.782	.860	.868	.355	.715	.794	.838
.355	.931	1.007	.944	.355	.858	.935	.907	.430	.799	.877	.880
.405	1.033	1.101	.986	.405	.905	.981	.924	.510	.861	.940	.908
.455	1.041	1.110	.991	.455	.955	1.027	.948	.555	.911	.986	.933
.505	1.057	1.127	.998	.505	.977	1.043	.958	.605	.935	1.006	.944
.555	1.054	1.120	1.003	.555	.999	1.063	.968	.655	.982	1.051	.964
.605	1.062	1.127	1.000	.605	1.031	1.102	.984	.708	.991	1.062	.970
.655	1.074	1.146	1.008	.655	1.041	1.111	.988	.769	1.020	1.092	.982
.705	1.013	1.081	.978	.705	1.064	1.133	1.001	.808	1.046	1.117	.991
.755	.980	1.052	.964	.755	1.061	1.129	.997	.855	1.046	1.116	.991
.805	.952	1.024	.955	.805	1.059	1.127	.998	.905	1.065	1.132	.998
				.850	1.061	1.123	.997	.950	1.064	1.130	1.001
								1.016	1.087	1.133	1.000
								1.505	1.065	1.131	.999

STATION 4

$$a/L=0.400$$

$$\delta=1.35 \text{ inches}$$

0.005	0.110	0.175	0.395	0.005	0.100	0.163	0.381	0.005	0.083	0.146	0.366
.006	.124	.194	.415	.006	.118	.181	.403	.006	.097	.159	.379
.007	.159	.216	.439	.007	.140	.203	.427	.007	.122	.188	.412
.008	.175	.230	.455	.008	.165	.219	.441	.008	.137	.196	.421
.009	.190	.245	.466	.009	.185	.241	.465	.009	.143	.206	.433
.010	.211	.266	.488	.010	.192	.248	.470	.010	.170	.224	.451
.011	.216	.274	.494	.011	.208	.262	.490	.011	.177	.229	.457
.012	.230	.284	.504	.012	.220	.276	.498	.012	.199	.248	.474
.013	.234	.291	.510	.013	.232	.286	.508	.013	.202	.256	.482
.014	.236	.289	.508	.014	.228	.282	.504	.015	.216	.269	.479
.015	.248	.304	.520	.015	.237	.291	.511	.019	.211	.265	.490
.017	.269	.315	.530	.016	.245	.297	.516	.021	.236	.289	.511
.020	.276	.331	.542	.017	.252	.306	.527	.025	.256	.311	.531
.025	.297	.352	.560	.018	.247	.306	.519	.030	.276	.328	.544
.035	.326	.377	.579	.020	.268	.322	.539	.035	.288	.340	.556
.050	.368	.420	.611	.022	.274	.330	.545	.045	.324	.375	.583
.075	.411	.466	.645	.025	.286	.337	.550	.055	.357	.409	.610
.105	.451	.508	.674	.030	.303	.356	.564	.080	.387	.442	.633
.205	.555	.609	.739	.040	.330	.382	.584	.105	.436	.488	.666
.305	.730	.784	.838	.056	.374	.427	.617	.156	.470	.526	.691
.405	.839	.893	.893	.080	.414	.468	.650	.205	.531	.588	.730
.505	.975	1.017	.955	.105	.440	.493	.666	.257	.575	.629	.745
.605	1.008	1.047	.966	.181	.526	.581	.723	.305	.654	.705	.800
1.008	1.031	1.072	.983	.305	.630	.686	.764	.405	.690	.742	.820
1.107	1.051	1.093	.988	.455	.736	.785	.839	.505	.760	.811	.855
1.205	1.059	1.097	.990	.605	.846	.895	.896	.655	.871	.918	.908
1.506	1.071	1.112	1.000	.855	.989	1.033	.963	.809	.955	1.003	.952
2.005	1.064	1.103	.994	.955	1.011	1.053	.971	1.005	1.031	1.077	.990
2.105	1.068	1.108	.996	1.065	1.049	1.090	.990	1.205	1.093	1.103	1.001
2.205	1.068	1.106	.998	1.305	1.071	1.109	.998	1.406	1.062	1.103	1.000
				1.505	1.068	1.102	.995	1.505	1.062	1.104	1.000
				1.706	1.071	1.106	.997	1.705	1.068	1.095	.998
				.705	.906	.953	.924	1.906	1.062	1.104	1.012

TABLE I—Continued

STATION 5

$a/L=0.505$

$\delta=1.71$ inches

Average $q_0=25.6$ lb./sq. ft.				$q_0=19.0$ lb./sq. ft.				$q_0=12.5$ lb./sq. ft.			
y inch	$\frac{H}{q_0}$	$\frac{q}{q_0}$	$\frac{u}{u_0}$	y inch	$\frac{H}{q_0}$	$\frac{q}{q_0}$	$\frac{u}{u_0}$	y inch	$\frac{H}{q_0}$	$\frac{q}{q_0}$	$\frac{u}{u_0}$
0.005	0.067	0.123	0.334	0.005	0.054	0.107	0.310	0.005	0.037	0.095	0.294
.006	.082	.136	.351	.006	.077	.132	.344	.006	.056	.113	.318
.007	.129	.183	.407	.007	.105	.160	.379	.007	.076	.134	.348
.008	.166	.220	.445	.008	.136	.191	.413	.008	.116	.171	.392
.009	.183	.237	.463	.009	.160	.211	.435	.009	.134	.189	.413
.010	.193	.247	.473	.010	.185	.238	.463	.010	.169	.224	.450
.011	.207	.260	.486	.011	.200	.254	.477	.011	.177	.232	.457
.012	.218	.270	.495	.012	.208	.263	.486	.012	.182	.251	.476
.013	.224	.278	.500	.013	.215	.270	.493	.013	.204	.261	.485
.014	.232	.284	.509	.014	.224	.281	.502	.014	.210	.269	.492
.015	.245	.299	.520	.015	.234	.289	.510	.015	.220	.270	.495
.017	.252	.306	.525	.017	.245	.302	.521	.016	.228	.283	.508
.020	.273	.325	.543	.020	.257	.314	.531	.017	.236	.295	.516
.025	.284	.339	.553	.025	.282	.340	.552	.020	.241	.301	.522
.035	.318	.375	.583	.035	.313	.372	.579	.025	.266	.326	.542
.045	.346	.405	.605	.055	.356	.417	.611	.037	.294	.354	.565
.055	.362	.423	.618	.080	.397	.460	.644	.055	.341	.405	.602
.105	.442	.507	.677	.105	.431	.485	.666	.080	.390	.455	.640
.155	.600	.565	.715	.155	.483	.552	.704	.107	.415	.481	.659
.205	.637	.602	.738	.205	.527	.595	.732	.155	.473	.542	.700
.405	.662	.726	.810	.306	.598	.660	.770	.205	.519	.586	.727
.606	.780	.836	.870	.505	.698	.763	.828	.305	.586	.652	.769
.809	.873	.924	.914	.705	.808	.868	.884	.505	.694	.763	.827
1.005	.943	.992	.947	.905	.910	.966	.933	.705	.800	.862	.882
1.206	1.003	1.059	.974	1.105	.971	1.024	.955	.905	.858	.944	.923
1.405				1.205	1.021	1.077	.968	1.105	.968	1.020	.958
1.405	1.047	1.089	.992	1.306	1.031	1.084	.977	1.206	.968	1.050	.972
1.505	1.049	1.092	.993	1.406	1.042	1.097	.988	1.305	1.024	1.077	.986
1.605	1.060	1.105	1.001	1.505	1.046	1.097	.991	1.405	1.040	1.094	.992
1.705	1.063	1.107	1.001	1.755	1.058	1.109	.998	1.505	1.049	1.100	.995
1.907	1.061	1.105	1.001	2.005	1.053	1.111	.996	1.755	1.055	1.109	1.000
2.205	1.061	1.102	.999	2.505	1.059	1.112	.996	2.005	1.059	1.113	1.000
2.505	1.061	1.104	1.001					2.505	1.069	1.116	1.001
3.005	1.053	1.104	1.000								

STATION 6

$a/L=0.590$

$\delta=1.93$ inches

0.005	0.063	0.136	0.347	0.005	0.051	0.121	0.331	0.005	0.033	0.105	0.309
.006	.086	.140	.353	.006	.081	.132	.344	.006	.040	.113	.320
.007	.082	.155	.371	.007	.089	.161	.380	.007	.063	.136	.351
.008	.121	.195	.416	.008	.126	.196	.419	.008	.093	.166	.388
.009	.148	.221	.443	.009	.141	.211	.435	.009	.123	.196	.421
.010	.157	.229	.451	.010	.160	.231	.455	.010	.141	.214	.438
.011	.177	.249	.470	.012	.183	.254	.476	.011	.160	.233	.455
.012	.189	.262	.483	.013	.199	.268	.490	.012	.171	.243	.467
.013	.200	.272	.493	.014	.201	.270	.490	.013	.186	.257	.480
.014	.209	.281	.500	.015	.216	.288	.506	.014	.193	.265	.489
.015	.220	.292	.509	.016	.217	.290	.509	.015	.200	.273	.496
.017	.231	.304	.520	.018	.228	.299	.516	.017	.207	.280	.502
.020	.244	.317	.530	.021	.238	.310	.526	.021	.230	.303	.523
.025	.259	.335	.545	.025	.254	.326	.540	.026	.248	.323	.540
.037	.290	.368	.571	.038	.294	.367	.574	.035	.274	.348	.560
.055	.345	.405	.612	.055	.330	.403	.601	.055	.315	.389	.592
.085	.400	.478	.652	.083	.378	.454	.638	.080	.364	.439	.629
.105	.424	.503	.667	.106	.419	.496	.667	.107	.391	.469	.650
.155	.475	.554	.702	.155	.458	.536	.693	.157	.472	.550	.704
.205	.519	.600	.731	.205	.506	.586	.725	.209	.506	.584	.725
.305	.684	.685	.789	.305	.579	.653	.766	.305	.543	.623	.748
.505	.656	.733	.808	.505	.634	.759	.825	.508	.668	.745	.818
.706	.778	.850	.871	.706	.772	.844	.868	.705	.753	.825	.861
.907	.856	.924	.907	.908	.836	.906	.900	.908	.833	.904	.901
1.215	.982	1.013	.951	1.105	.921	.986	.938	1.105	.916	.983	.941
1.405	1.009	1.068	.977	1.305	.976	1.040	.962	1.358	.985	1.050	.972
1.505	1.020	1.086	.984	1.507	1.026	1.091	.987	1.455	1.003	1.068	.981
1.605	1.028	1.019	.987	1.605	1.027	1.091	.988	1.557	1.039	1.101	.995
1.706	1.057	1.120	1.000	1.708	1.033	1.094	.988	1.655	1.044	1.110	.999
1.855	1.060	1.125	1.000	1.855	1.051	1.116	.997	1.805	1.050	1.116	1.000
2.005	1.060	1.124	.998	2.005	1.055	1.118	.999	2.005	1.051	1.117	1.000
2.506	1.068	1.132	1.000	2.505	1.058	1.119	1.000	2.505	1.064	1.128	1.007

STATION 7

$a/L=0.679$

$\delta=2.33$ inches

0.005	0.038	0.110	0.313	0.005	0.031	0.107	0.309	0.005	0.014	0.086	0.276
.006	.049	.123	.331	.006	.042	.117	.320	.006	.030	.104	.304
.007	.078	.163	.368	.007	.073	.147	.362	.007	.052	.126	.338
.008	.117	.191	.413	.008	.102	.176	.396	.008	.083	.157	.375
.009	.124	.198	.421	.009	.128	.202	.424	.009	.109	.184	.405
.010	.146	.220	.443	.011	.150	.224	.446	.010	.119	.193	.417
.011	.157	.232	.453	.012	.161	.235	.456	.011	.137	.211	.436
.012	.171	.246	.467	.013	.174	.248	.467	.012	.152	.225	.452
.013	.182	.257	.478	.014	.187	.261	.478	.013	.169	.232	.460
.014	.190	.265	.486	.015	.189	.262	.482	.014	.168	.242	.467
.015	.198	.272	.493	.018	.202	.276	.494	.015	.178	.251	.476
.017	.210	.284	.503	.020	.210	.283	.501	.017	.190	.263	.487

TABLE I—Continued
STATION 7—Continued

Average $q_0=25.6$ lb./sq. ft.				$q_0=19.0$ lb./sq. ft.				$q_0=12.5$ lb./sq. ft.			
y inch	$\frac{H}{q_0}$	$\frac{q}{q_0}$	$\frac{u}{u_1}$	y inch	$\frac{H}{q_0}$	$\frac{q}{q_0}$	$\frac{u}{u_1}$	y inch	$\frac{H}{q_0}$	$\frac{q}{q_0}$	$\frac{u}{u_1}$
0.021	0.226	0.300	0.518	0.025	0.228	0.302	0.516	0.021	0.211	0.284	0.507
.025	.241	.315	.530	.035	.255	.330	.539	.026	.233	.306	.527
.035	.272	.348	.558	.055	.315	.392	.591	.037	.253	.328	.546
.055	.314	.390	.589	.080	.351	.428	.614	.056	.300	.374	.582
.085	.367	.445	.629	.108	.390	.468	.641	.083	.341	.416	.612
.120	.407	.486	.659	.155	.420	.497	.665	.106	.365	.441	.631
.155	.437	.518	.680	.205	.478	.559	.708	.156	.423	.502	.671
.205	.480	.560	.707	.405	.588	.665	.768	.209	.461	.539	.697
.405	.574	.653	.783	.658	.694	.764	.820	.405	.577	.655	.765
.658	.683	.772	.830	.911	.793	.861	.872	.607	.666	.742	.815
.905	.804	.875	.886	1.205	.886	.953	.920	.905	.776	.847	.869
1.205	.898	.967	.929	1.505	.971	1.039	.956	1.205	.879	.948	.921
1.505	.959	1.024	.955	1.605	.976	1.043	.963	1.505	.942	1.006	.951
1.655	1.004	1.069	.978	1.705	1.007	1.073	.975	1.605	.987	1.052	.966
1.805	1.024	1.090	.988	1.805	1.017	1.082	.984	1.705	.986	1.051	.971
2.005	1.045	1.110	.998	2.005	1.034	1.103	.989	1.805	1.016	1.082	.978
2.305	1.053	1.118	1.000	2.309	1.058	1.125	.994	2.108	1.047	1.113	.991
2.605	1.053	1.118	1.000	2.609	1.068	1.137	.999	2.405	1.056	1.123	1.000
3.005	1.057	1.122	1.002	3.005	1.068	1.137	1.001	2.705	1.060	1.124	1.000
								3.005	1.062	1.126	1.000

STATION 8

$$a/L=0.775$$

$$\delta=3.17 \text{ inches}$$

0.005	0.057	0.095	0.295	0.005	0.055	0.091	0.290	0.005	0.032	0.067	0.250
.006	.064	.101	.303	.006	.058	.095	.296	.006	.047	.083	.290
.007	.065	.121	.333	.007	.073	.110	.318	.007	.051	.088	.286
.008	.116	.182	.373	.008	.099	.136	.354	.009	.101	.136	.355
.010	.146	.183	.408	.009	.123	.160	.385	.010	.111	.146	.368
.011	.157	.194	.422	.010	.136	.173	.401	.011	.125	.161	.385
.012	.166	.202	.429	.011	.145	.182	.411	.013	.151	.187	.416
.013	.179	.215	.445	.012	.155	.190	.418	.014	.156	.193	.422
.014	.187	.224	.452	.013	.165	.200	.430	.015	.168	.204	.434
.015	.191	.228	.456	.014	.176	.213	.444	.017	.179	.214	.446
.017	.200	.236	.464	.015	.186	.224	.454	.020	.193	.220	.460
.020	.210	.248	.475	.018	.197	.234	.466	.027	.211	.246	.478
.025	.233	.269	.497	.021	.211	.248	.479	.038	.230	.264	.495
.035	.255	.293	.516	.027	.223	.261	.491	.055	.260	.296	.523
.058	.288	.326	.546	.036	.244	.283	.510	.081	.294	.332	.555
.082	.327	.366	.579	.055	.286	.325	.546	.105	.326	.363	.581
.105	.355	.395	.599	.080	.307	.347	.562	.105	.370	.409	.616
.159	.398	.439	.631	.106	.334	.394	.605	.215	.408	.444	.643
.206	.427	.468	.653	.156	.386	.425	.627	.415	.503	.545	.711
.406	.651	.693	.734	.205	.416	.458	.651	.655	.594	.632	.767
.655	.636	.672	.785	.405	.539	.670	.729	.905	.699	.730	.822
.905	.727	.760	.836	.655	.621	.661	.785	1.205	.766	.797	.861
1.205	.817	.850	.882	.905	.701	.734	.820	1.507	.850	.882	.903
1.506	.833	.911	.913	1.305	.817	.850	.885	1.765	.876	.907	.917
1.605	.907	.935	.925	1.607	.867	.897	.906	2.018	.954	.983	.955
1.805	.948	.975	.947	1.705	.935	.963	.945	2.255	.996	1.026	.978
2.005	.988	1.021	.965	1.905	.951	.979	.953	2.508	1.017	1.043	.987
2.206	.992	1.020	.968	2.105	.982	1.010	.969	2.755	1.041	1.068	.994
2.405	1.020	1.013	.980	2.405	1.028	1.050	.983	3.013	1.053	1.070	.999
2.706	1.057	1.089	.997	2.705	1.050	1.080	1.000	3.515	1.053	1.070	1.000
3.005	1.057	1.089	.997	3.005	1.050	1.079	.997				
3.506	1.056	1.088	1.003	3.705	1.063	1.093	1.000				

STATION 9

$$a/L=0.869$$

$$\delta=4.67 \text{ inches}$$

0.005	0.107	0.062	0.246	0.005	0.103	0.059	0.240	0.005	0.082	0.041	0.201
.006	.118	.076	.273	.006	.114	.071	.262	.006	.097	.056	.235
.007	.134	.092	.299	.007	.131	.090	.296	.008	.117	.078	.276
.008	.146	.104	.318	.008	.143	.100	.313	.009	.127	.083	.286
.009	.168	.126	.350	.009	.157	.114	.335	.011	.157	.110	.331
.010	.174	.132	.359	.010	.163	.120	.343	.012	.163	.121	.344
.011	.182	.140	.372	.011	.175	.133	.360	.013	.168	.126	.352
.012	.187	.146	.378	.012	.183	.141	.372	.014	.176	.137	.368
.013	.193	.157	.392	.014	.199	.158	.393	.015	.187	.145	.378
.015	.207	.166	.403	.017	.206	.165	.402	.017	.194	.152	.388
.017	.212	.171	.409	.020	.216	.176	.416	.020	.203	.161	.399
.020	.222	.181	.424	.025	.221	.179	.418	.025	.218	.176	.417
.025	.233	.193	.434	.036	.247	.203	.451	.035	.227	.190	.434
.035	.246	.210	.453	.055	.264	.220	.470	.065	.269	.224	.480
.059	.284	.250	.494	.105	.314	.279	.523	.114	.289	.254	.500
.107	.325	.293	.540	.206	.371	.339	.576	.211	.377	.344	.534
.205	.378	.348	.581	.410	.451	.419	.640	.407	.430	.393	.637
.405	.464	.431	.649	.656	.628	.494	.698	.653	.610	.476	.686
.655	.635	.502	.699	.905	.696	.568	.740	.906	.683	.548	.736
.905	.610	.571	.748	1.206	.644	.604	.770	1.204	.668	.629	.789
1.205	.679	.640	.790	1.605	.750	.711	.834	1.605	.728	.687	.825
1.705	.788	.748	.854	2.005	.831	.793	.852	2.005	.812	.772	.874
2.205	.872	.831	.900	2.506	.919	.878	.929	2.507	.918	.876	.929
2.711	.942	.902	.937	3.008	.997	.955	.985	3.010	.983	.945	.966
3.205	.996	.955	.964	3.510	1.025	.985	.983	3.605	1.038	1.001	.993
3.705	1.055	1.012	.994	4.011	1.051	1.008	.994	4.006	1.043	1.001	.995
4.005	1.053	1.012	.994	4.302	1.061	1.020	.998	4.305	1.048	1.002	.995
4.305	1.057	1.017	.996	4.610	1.058	1.018	.996	4.607	1.052	1.010	1.000
4.705	1.062	1.025	1.000	5.012	1.065	1.023	1.001	5.005	1.055	1.017	1.002
5.005	1.061	1.025	1.000	5.405	1.065	1.023	1.001	5.510	1.053	1.013	1.000